

Ecological and evolutionary implications of starvation and body size

1 **Justin D. Yeakel * †‡, Christopher P. Kempes †, and Sidney Redner †§**

4 *School of Natural Science, University of California Merced, Merced, CA, †The Santa Fe Institute, Santa Fe, NM, §Department of Physics, Boston University, Boston
5 MA, and ‡To whom correspondence should be addressed: jdyeakel@gmail.com

6 Submitted to Proceedings of the National Academy of Sciences of the United States of America

7 **This is the abstract.** No it isn't. It's merely a placeholder.

8 foraging | starvation | reproduction

9 Introduction

10 The behavioral ecology of most, if not all, organisms is influ-
11 enced by the energetic state of individuals, which directly influ-
12 ences how organisms invest reserves in uncertain environments.
13 Such behaviors are generally manifested as trade-offs between
14 investing in somatic maintenance and growth or allocating en-
15 ergy towards reproduction [1, 2, 3]. The timing of these be-
16 haviors responds to selective pressure, as the choice of the in-
17 vestment impacts future fitness! [4]. The influence of resource
18 limitation on an organism's ability to maintain its nutritional
19 stores may lead to repeated delays or shifts in reproduction over
20 the course of an organism's life.

21 The life history of most species is typically comprised of (a)
22 somatic growth and maintenance and (b) reproduction. The
23 balance between these two activities is often conditioned on
24 resource availability [5]. For example, reindeer invest less in
25 calves born after harsh winters (when the mother's energetic
26 state is depleted) than in calves born after moderate winters [6].
27 Many bird species invest differently in broods during periods
28 of resource scarcity compared to normal periods [7, 8], some-
29 times delaying or even foregoing reproduction for a breeding
30 season [1, 9, 10]. Even freshwater and marine zooplankton have
31 been observed to avoid reproduction under nutritional stress
32 [11], and those that do reproduce have lower survival rates [2].
33 Organisms may also separate maintenance and growth from re-
34 production over space and time: many salmonids, birds, and
35 some mammals return to migratory breeding grounds to repro-
36 duce after one or multiple seasons in resource-rich environments
37 where they accumulate nutritional reserves [12, 13, 14].

38 Physiological mechanisms also play an important role in reg-
39 ulating reproductive expenditures during periods of resource
40 limitation. Diverse mammals (47 species in 10 families) ex-
41 hibit delayed implantation, whereby females postpone fetal
42 development (blastocyst implantation) until times where nu-
43 tritional reserves can be accumulated [15, 16]. Many other
44 many species (including humans) suffer irregular menstrual cy-
45 cling and higher abortion rates during periods of nutritional
46 stress [17, 18]. In the extreme case of unicellular organisms,
47 nutrition is unavoidably linked to reproduction because the nu-
48 tritional state of the cell regulates all aspects of the cell cycle
49 [19]. The existence of so many independently evolved mechan-
50 isms across such a diverse suite of organisms highlights the im-
51 portance and universality of the fundamental tradeoff between
52 somatic and reproductive investment. However the dynamic
53 implications of these constraints are unknown.

54 Though straightforward conceptually, incorporating the en-
55 ergetic dynamics of individuals [20] into a population-level
56 framework [20, 21] presents numerous mathematical obsta-
57 cles [22]. An alternative approach involves modeling the
58 macroscale relations that guide somatic versus reproductive
59 investment in a consumer-resource system. For example,
60 macroscale Lotka-Volterra models assume that the growth rate

61 of the consumer population depends on resource density, thus
62 *implicitly* incorporating the requirement of resource availability
63 for reproduction [23].

64 In this work, we adopt an alternative approach in which re-
65 source limitation and the subsequent effect of starvation is ac-
66 counted for *explicitly*. Namely, only individuals with sufficient
67 energetic reserves can reproduce. Such a constraint leads to
68 reproductive time lags due to some members of the population
69 starving and then recovering. Additionally, we incorporate the
70 idea that reproduction is strongly constrained allometrically [3],
71 and is not generally linearly related to resource density. As we
72 shall show, these constraints influence the ensuing population
73 dynamics in dramatic ways.

74 Nutritional-state-structured model (NSM)

75 We begin by defining a minimal Nutritional-State-
76 structured population Model (NSM), where the consumer pop-
77 ulation is divided into two energetic states: (a) an energetically
78 replete (full) state F , where the consumer reproduces at a con-
79 stant rate λ , and (b) an energetically deficient (hungry) state
80 H , where the consumer does not reproduce but dies at rate μ .
81 The underlying resource R evolves by logistic growth with an
82 intrinsic growth rate α and a carrying capacity equal to one.
83 Consumers transition from the full state F to the hungry state
84 H by starvation at rate σ and also in proportion to the absence
85 of resources $(1 - R)$. Conversely, consumers recover from state
86 H to state F at rate ρ and in proportion to R . Resources are
87 also eaten by the consumers—at rate ρ by hungry consumers
88 and at rate $\beta < \rho$ by full consumers. This inequality accounts
89 for hungry consumers requiring more resources to rebuild body
90 weight.

90 In the mean-field approximation, in which the consumers
91 and resources are perfectly mixed, their densities evolve accord-
92 ing to the rate equations

$$\begin{aligned}\dot{F} &= \lambda F + \rho RH - \sigma(1 - R)F, \\ \dot{H} &= \sigma(1 - R)F - \rho RH - \mu H, \\ \dot{R} &= \alpha R(1 - R) - R(\rho H + \beta F).\end{aligned}\quad [1]$$

93 Notice that the total consumer density $F + H$ evolves accord-
94 ing to $\dot{F} + \dot{H} = \lambda F - \mu H$. This resembles the equation of
95 motion for the predator density in the classic Lotka-Volterra
96 model, except that the resource density does not appear in the

Reserved for Publication Footnotes

99 growth term. As discussed above, the attributes of reproduction and mortality have been explicitly apportioned to the full 100 and hungry consumers, respectively, so that the growth in the total density is decoupled from the resource density.

103 Equation [1] has three fixed points: two trivial fixed points at $(F^*, H^*, R^*) = (0, 0, 0)$ and $(0, 0, 1)$, and one non-trivial, 104 internal fixed point at

$$\begin{aligned} F^* &= \frac{\alpha\lambda\mu(\mu + \rho)}{(\lambda\rho + \mu\sigma)(\lambda\rho + \mu\beta)}, \\ H^* &= \frac{\alpha\lambda^2(\mu + \rho)}{(\lambda\rho + \mu\sigma)(\lambda\rho + \mu\beta)}, \\ R^* &= \frac{\mu(\sigma - \lambda)}{\lambda\rho + \mu\sigma}. \end{aligned}$$

106 If this internal fixed point, which is unique, is stable, it will 107 be the global attractor for all population trajectories for any 108 initial condition where the resource and consumer densities are 109 both non zero. The stability of this fixed point is determined by 110 the Jacobian Matrix \mathbf{J} , where each matrix element J_{ij} equals 111 $\partial\dot{X}_i/\partial X_j$ when evaluated at the internal fixed point, and \mathbf{X} is 112 the vector (F, H, R) . If the parameters in Eq. [1] are such that 113 the real part of the largest eigenvalue of \mathbf{J} is negative, then the 114 system is stable with respect to small perturbations from the 115 fixed point.

116 From Eq. [2], an obvious constraint on the NSM is that 117 the reproduction rate λ must be less than the starvation rate 118 σ , so that R^* is positive. Moreover, when the resource density 119 $R = 0$, the rate equation for F gives exponential growth for 120 $\lambda > \sigma$. The condition $\sigma = \lambda$ represents a transcritical (TC) bi- 121 furcation that demarcates the physical and unphysical regimes. 122 The biological implication of the constraint $\lambda < \sigma$ is simple— 123 the rate at which a macroscopic organism loses mass due to 124 lack of resources is generally much faster than the rate of repro- 125 duction. As we will discuss below, this inequality is a natural 126 consequence of allometric constraints [3] for organisms within 127 empirically observed body size ranges (Fig. 2).

128 In the physical regime of $\lambda < \sigma$, the fixed point [2] may 129 either be a stable node or a limit cycle (Fig. 3). In continuous- 130 time systems, a limit cycle arises when a pair of complex con- 131 jugate eigenvalues crosses the imaginary axis to attain positive 132 real parts [24]. This Hopf bifurcation is defined by $\text{Det}(\mathbf{S}) = 0$, 133 where \mathbf{S} is the Sylvester matrix, which is composed of the co- 134 efficients of the characteristic polynomial of the Jacobian ma- 135 trix [25]. As the system parameters are tuned to be within the 136 stable regime but close to the Hopf bifurcation, the amplitude 137 of the transient but decaying cycles become large. Given that 138 ecological systems are constantly being perturbed [26], the on- 139 set of transient cycles, even though they decay with time, can 140 increase the extinction risk [27, 28, 29]. Thus the distance of 141 a system from the Hopf bifurcation provides a measure of its 142 persistence.

143 When the starvation rate $\sigma \gg \lambda$, a substantial fraction 144 of the consumers are driven to the hungry non-reproductive 145 state. Because reproduction is inhibited, there is a low steady- 146 state consumer density and a high steady-state resource density. 147 However, if σ/λ approaches one, the population is overloaded 148 with energetically-replete (reproducing) individuals, thereby 149 promoting oscillations between the consumer and resource den- 150 sities (Fig. 3).

151 Whereas the consumer growth rate λ defines an absolute 152 bound of biological feasibility—the TC bifurcation—the star- 153 vation rate σ determines the sensitivity of the consumer popu- 154 lation to changes in resource density. When $\sigma \gg \lambda$, the steady- 155 state population density is small, thereby increasing the risk of 156 stochastic extinction. Conversely, as σ decreases, the system 157 will ultimately be poised either near the TC or the Hopf bi-

158 furcation (Fig. 3). If the recovery rate ρ is sufficiently small, 159 the TC bifurcation is reached and the resource eventually is 160 eliminated. If ρ exceeds a threshold value, cyclic dynamics will 161 develop as the Hopf bifurcation is approached.

162 Role of allometry

163 The NSM describes a broad range of dynamics, yet organisms 164 are likely unable to access most of the total parameter space. 165 Here we use allometric scaling relationships to constrain the 166 covariation of rates in a principled and biologically meaning- 167 ful manner. Allometric scaling relationships highlight common 168 constraints and average trends across large ranges in body size 169 and species diversity. Many of these relationships can be de- 170 rived from a small set of assumptions and below we describe 171 a framework for the covariation of timescales and rates across 172 the range of mammals for each of the key parameters of our 173 model (cf. [30]). We are able to define the regime of dynam- 174 ics occupied by the entire class of mammals along with the key 175 differences between the largest and smallest mammals.

176 Nearly all of the rates described in the NSM are to some 177 extent governed by consumer metabolism, which can be used 178 to describe a variety of organism features []. The scaling rela- 179 tionship between an organism's metabolic rate B and its body 180 size at reproductive maturity M is well documented [31] and 181 scales as $B = B_0 M^\eta$, where η is the scaling exponent, gener- 182 ally assumed to vary around 2/3 or 3/4 for metazoans [], and 183 has taxonomic shifts for unicellular species between $\eta \approx 1$ in 184 eukaryotes and $\eta \approx 1.76$ in bacteria [32, 3]. Several efforts have 185 shown how a partitioning of this metabolic rate between growth 186 and maintenance purposes can be used to derive a general equa- 187 tion for the growth trajectories and growth rates of organisms 188 ranging from bacteria to metazoans [3, ?]. More specifically, 189 the interspecific trends in growth rate can be approximated by

$$\lambda = \lambda_0 M^{\eta-1}. \quad [3]$$

190 This relationship is derived from the simple balance

$$B_0 m^\eta = E_m \frac{dm}{dt} + B_m m \quad [4]$$

191 where E_m is the energy needed to synthesize a unit of mass, 192 B_m is the metabolic rate to support an existing unit of mass, 193 and m is the mass at any point in development. It is useful to 194 explicitly write this balance because it can also be modified to 195 understand the timescales of both starvation and recovery from 196 starvation as we show below.

197 For the rate of starvation, σ , we are interested in the time 198 that it takes an organism to go from healthy adulthood to a 199 smaller size where reproduction is impossible. This process is 200 defined by the energy balance in Equation 4 where we make the 201 simple assumption that an organism must meet its maintenance 202 requirements using the digestion of existing mass as the sole 203 energy source. This assumption implies the simple metabolic

$$\frac{dm}{dt} E'_m = -B_m m \quad [5]$$

205 where E'_m is the amount of energy stored in a unit of exist- 206 ing body mass which differs from E_m [], the energy required to 207 synthesis a unit of biomass. Given the adult mass, M , of an 208 organism this energy balance prescribes the mass trajectory of 209 a starving organism:

$$m(t) = M e^{-B_m t / E'_m}. \quad [6]$$

210 Considering that only certain tissues can be digested for energy, 211 for example the brain cannot be degraded to fuel metabolism, 212 we define the rate for starvation and death by the timescales

required to reach specific fractions of normal adult mass. We mean; Fig. 4) results in little qualitative difference. These define $m_{starve} = \epsilon M$, where $\epsilon < 1$ is the fraction of adult mass where reproduction ceases. This fraction will change if oscillations – including both stable limit cycles as well as transient tissue composition systematically scales with adult mass. For sient cycles – than mammals with larger body size. Our model example, considering the observation that body fat in mammals scales with overall body size according to $M_f = f_0 M^\gamma$, and as suming that once this mass is fully digested the organism begins to starve, would imply that $\epsilon = 1 - f_0 M^\gamma / M$. Taken together the time scale for starvation is given by

$$t_\sigma = -\frac{E_m \log(\epsilon)}{B_m}. \quad [6]$$

The starvation rate is then $\sigma = 1/t_\sigma$, which will scale with adult mass following $1/\log(1 - f_0 M^\gamma / M)$. In either case σ does not have a simple scaling with λ (Equation 3) which is important for the dynamics that we later discuss.

The time to death should follow a similar relationship, but defined by a lower fraction of adult mass, $m_{death} = \epsilon' M$. Consider, for example, that an organism dies once it has digested all fat and muscle tissues, and that muscle tissue scales with body mass according to $M_{mm} = mm_0 M^\zeta$, then $\epsilon' = 1 - (f_0 M^\gamma + mm_0 M^\zeta) / M$. Muscle mass has been shown to be roughly proportional to body mass [33] in mammals and thus ϵ' is effectively ϵ minus a constant. Thus

$$t_\mu = -\frac{E_m \log(\epsilon')}{B_m}. \quad [7]$$

and $\mu = 1/t_\mu$.

The rate of recovery $\rho = 1/t_\rho$ requires that an organism accrues tissue from the starving state to the full state. We again use the balance given in Equation 4 to find the timescale to return to the mature mass from a given reduced starvation mass. The solution to Equation 4 is given by

$$m(t) = \left(\frac{B_0}{B_m} \right)^{1/(\eta-1)} \left[1 - \left(1 - \frac{B_m}{B_0} m_0^{1-\eta} \right) e^{-b(1-\eta)t} \right]^{1/(1-\eta)}.$$

We are then interested in the timescale, $t_\rho = t_2 - t_1$, which is the time it takes to go from $m(t_1) = \epsilon M$ to $m(t_2) = M$, or

$$t_\rho = \frac{E_m \left(\log \left(1 - \frac{B_0}{B_m} (M)^{1-\eta} \right) - \log \left(1 - \frac{B_0}{B_m} (\epsilon M)^{1-\eta} \right) \right)}{(\eta-1)B_m}.$$

Although these rate equations are general, here we focus on parameterizations for terrestrial-bound endotherms, specifically mammals, which range from $M \approx 1$ gram (the Etruscan shrew *Suncus etruscus*) to $M \approx 10^7$ grams (the late Eocene to early Miocene Indricotheriinae). Investigating other classes of organisms would simply involve altering the metabolic exponents and scalings associate with ϵ . Moreover, we emphasize that our allometric equations describe mean relationships, and do not account for the (sometimes considerable) variance associated with individual species.

The stabilizing effects of allometric constraints

As the allometric derivations of NSM rate laws reveal, σ and ρ are not independent parameters, and the bifurcation space shown in Fig. 3 is navigated via covarying parameters. Given the parameterization for terrestrial endotherms we find that σ and ρ are constrained to a small window of potential values (Fig. 4) for the known range of body sizes M . We find that the dynamics for all mammalian body sizes is confined to the steady-state regime which does not contain limit cycles. Moreover, for larger M , the distance to the Hopf bifurcation increases, while uncertainty in allometric parameters (20% variation around the

Previous studies have used allometric constraints explain the periodicity of cyclic populations [34, 35, 36], suggesting a period $\propto M^{0.25}$, however this relationship seems to hold only for some species [37] and competing explanations [related to] exist [38, 39]. Statistically significant support for the existence of population cycles among mammals is predominantly based on time-series for smaller bodied mammals [40], where we our model would predict much longer and more pronounced transient dynamics given how close these points are to the Hopf bifurcation. We acknowledge that longer generation times, and more difficult measurement procedures, precludes similar quality data for larger organisms.

Extinction risk Within our model higher rates of starvation result in a larger flux of the population to the hungry state, eliminating reproduction and increasing the likelihood of mortality. However, from the perspective of population survival, it is the rate of starvation relative to the rate of recovery that determines the long-term dynamics of the system (Fig 3). We examine the competing effects of cyclic dynamics vs. changes in steady state density on extinction risk as a function of the ratio σ/ρ . We computed the probability of extinction, where extinction is assumed if the population trajectory goes below $0.2 \times$ the allometrically constrained steady state across all values of $10^2 < t \leq 10^6$, for 1000 replicates of the continuous-time system shown in Eq. 1 for an organism of $M = 100$ grams, assuming random initial conditions around the steady state (Eq. 2). By allowing the rate of starvation to vary, we assessed extinction risk across a range of values of the ratio σ/ρ varying between 10^{-2} to 2.5, thus examining a horizontal cross-section of Fig. 3. As expected, higher rates of extinction correlated with both low and high values of σ/ρ ; for low values the higher extinction risk results from transient cycles with larger amplitudes as the system nears the Hopf bifurcation (Fig. 5). For large values of σ/ρ , higher extinction risk is due to the decrease in the steady state consumer population density. This interplay creates an ‘extinction refuge’ as shown in Fig. 5, such that for a relatively constrained range of σ/ρ , extinction probabilities are minimized.

We find that the allometrically constrained values of σ/ρ (with $\pm 20\%$ variability around energetic parameter means) fall within the extinction refuge. These values are close enough to the Hopf bifurcation to avoid low steady state densities, and far enough away to avoid large-amplitude transient cycles. The fact that allometric values of σ and ρ fall within this relatively small window supports the possibility that a selective mechanism has constrained the physiological conditions driving observed starvation and recovery rates within populations. Such a mechanism would select for organism physiology that generates appropriate σ and ρ values that avoid extinction, and this could occur via the tuning of body fat percentages, metabolic rates, and biomass maintenance efficiencies. Nevertheless, our finding that the allometrically-determined parameters fall within this low extinction probability region suggests that the NSM dynamics may both drive – and constrain – natural animal populations.

Dynamic and energetic barriers to body size

Metabolite transportation constraints are widely thought to place strict boundaries on biological scaling [41, 42, 43], leading to specific predictions on the minimum possible body size

for organisms [44]. Above this bound, a number of energetic mechanisms have been explored to assess the costs and benefits associated with larger body masses, particularly for mammals. The *fasting endurance hypothesis* contends that larger body size, with lower metabolic rates and able to hold more endogenous energetic reserves, may buffer organisms against environmental fluctuations in resource availability [45]. Over evolutionary time, terrestrial mammalian lineages show a significant trend towards larger body size (known as Cope's Rule) [46, 47, 48, 49], and it is thought that drivers generate selection towards an optimal upper-bound of ca. 10⁷ grams [46], the value of which may arise from higher extinction risk for large taxa over evolutionary timescales [47].

These trends are thought to be driven by a combination of climate change and niche availability [49], however the underlying energetic costs and benefits of larger body sizes, and how they influence dynamics over ecological timescales, has not been explored, and we contend that the NSM provides a suitable framework to explore these issues.

A lower bound on mammalian body size is given by $\epsilon = 1/(B_0/B_m)^{1/(\eta-1)}$, where mammals have no reserves and immediately starve, which occurs at a size of $M = \text{value}$. This calculation gives an extreme limit on size but does not account for the subtleties of starvation dynamics that may limit body size. The NSM correctly predicts that species with smaller masses have larger steady-state population densities, however we observe that there is a sharp asymptote in both steady state densities as well as σ/ρ at $M \approx 0.3$ grams (Fig. 6a,b).

The rates of starvation and recovery explain why: as mass decreases, the rate of starvation increases, while the rate of recovery declines super-exponentially. This decline in ρ occurs when body fat percentage is $1 - 1/((B_0/B_m)^{1/(\eta-1)} M) \approx 2\%$, whereupon consumers have no eligible route out of starvation. Compellingly, this dynamic bound determined by the rate of energetic recovery is close to the minimum observed mammalian body size of ca. 1.3–2.5 grams (Fig. 6b,c), a range that occurs as the recovery rate begins its decline. In addition to known transport limitations [44], we suggest that an additional constraint of lower body size stems from the dynamics of starvation. This work mirrors other efforts where coincident limitations seem to limit the smallest possibilities for life within a particular class or organisms [?].

We examine a potential upper bound to body mass by assessing population invasibility with respect to a mutated sub-set of the population (denoted by $'$) where individuals have

The observed switch in invasibility as a function of χ at $M_{\text{opt}} \approx 10^6$ g thus serves as an attractor, where over evolutionary time the NSM predicts organismal mass to increase if $M < M_{\text{opt}}$ and decrease if $M > M_{\text{opt}}$. Moreover, M_{opt} , which is entirely determined by the population-level consequences of

energetic constraints is within an order of magnitude as that observed in the North American mammalian fossil record [46] and as that predicted from an evolutionary model of body size evolution [47]. While the state of the environment, as well as the competitive landscape, will determine whether specific body sizes are selected for or against [49], we suggest that the NSM correctly predicts that starvation dynamic proposed here may supply the fundamental momentum fueling the evolution of larger body size among terrestrial mammals.

The energetics associated with somatic maintenance, growth, and reproduction are important elements that influence the dynamics of all populations [9]. The NSM is a minimal and general model that incorporates the dynamics of starvation that are expected to occur in resource limited environments. By incorporating allometric relationships between the rates in the NSM, we find *i*) different organismal masses are more or less prone to different population dynamic regimes, *ii*) allometrically-determined rates of starvation and recovery appear to minimize extinction risk, and *iii*) the dynamic consequences of these rates may place additional barriers on the evolution of minimum and maximum body size. We suggest that the NSM offers a means by which the dynamic consequences of energetic constraints can be assessed using macroscale interactions between and among species. Future efforts will involve exploring the consequences of these dynamics in a spatially explicit framework, thus incorporating elements such as movement costs and spatial heterogeneity, which may elucidate additional tradeoffs associated with the dynamics of starvation.

1. Martin TE (1987) Food as a Limit on Breeding Birds: A Life-History Perspective. *Annu. Rev. Ecol. Syst.* 18:453–487.
2. Kirk KL (1997) Life-History Responses to Variable Environments: Starvation and Reproduction in Planktonic Rotifers. *Ecology* 78:434–441.
3. Kempes CP, Dutkiewicz S, Follows MJ (2012) Growth, metabolic partitioning, and the size of microorganisms. *PNAS* 109:495–500.
4. Mangel M, Clark CW (1988) *Dynamic Modeling in Behavioral Ecology* (Princeton University Press, Princeton).
5. Morris DW (1987) Optimal Allocation of Parental Investment. *Oikos* 49:332.
6. Tveraa T, Fauchald P, Henaug C, Yoccoz NG (2003) An examination of a compensatory relationship between food limitation and predation in semi-domestic reindeer. *Oecologia* 137:370–376.
7. Daan S, Dijkstra C, Drent R, Meijer T (1988) Food supply and the annual timing of avian reproduction.
8. Jacot A, Valcu M, van Oers K, Kempenaers B (2009) Experimental nest site limitation affects reproductive strategies and parental investment in a hole-nesting passerine. *Animal Behaviour* 77:1075–1083.
9. Stearns SC (1989) Trade-Offs in Life-History Evolution. *Funct. Ecol.* 3:259.
10. Barboza P, Jorde D (2002) Intermittent fasting during winter and spring affects body composition and reproduction of a migratory duck. *J Comp Physiol B* 172:419–434.
11. Threlkeld ST (1976) Starvation and the size structure of zooplankton communities. *Freshwater Biol.* 6:489–496.
12. Weber TP, Ens BJ, Houston AI (1998) Optimal avian migration: A dynamic model of fuel stores and site use. *Evolutionary Ecology* 12:377–401.
13. Mduma SAR, Sinclair ARE, Hilborn R (1999) Food regulates the Serengeti wildebeest: a 40-year record. *J. Anim. Ecol.* 68:1101–1122.
14. Moore JW, Yeakel JD, Peard D, Lough J, Beere M (2014) Life-history diversity and its importance to population stability and persistence of a migratory fish: steelhead in two large North American watersheds. *J. Anim. Ecol.*
15. Mead RA (1989) In *Carnivore Behavior, Ecology, and Evolution* (Springer US, Boston, MA), pp 437–464.
16. Sandell M (1990) The Evolution of Seasonal Delayed Implantation. *The Quarterly Review of Biology* 65:23–42.
17. Bulik CM, et al. (1999) Fertility and Reproduction in Women With Anorexia Nervosa. *J. Clin. Psychiatry* 60:130–135.
18. Trites AW, Donnelly CP (2003) The decline of Steller sea lions *Eumetopias jubatus* in Alaska: a review of the nutritional stress hypothesis. *Mammal Review* 33:3–28.
19. Glazier DS (2009) Metabolic level and size scaling of rates of respiration and growth in unicellular organisms. *Funct. Ecol.* 23:963–968.
20. Kooijman SALM (2000) *Dynamic Energy and Mass Budgets in Biological Systems* (Cambridge).
21. Sousa T, Domingos T, Poggiale JC, Kooijman SALM (2010) Dynamic energy budget theory restores coherence in biology. *Philos. T. Roy. Soc. B* 365:3413–3428.

- 463 22. Diekmann O, Metz JAJ (2010) How to lift a model for individual behaviour to the 496 38. Kendall BE, et al. (1999) Why do populations cycle? A synthesis of statistical and
464 population level? *Philos. T. Roy. Soc. B* 365:3523–3530. 497 mechanistic modeling approaches. *Ecology* 80:1789–1805.
- 465 23. Murdoch WW, Briggs CJ, Nisbet RM (2003) *Consumer-resource Dynamics*, Mono- 498 39. Höglstedt G, Seldal T, Breistol A (2005) Period length in cyclic animal populations.
466 graphs in population biology (Princeton University Press). 499 *Ecology* 86:373–378.
- 467 24. Guckenheimer J, Holmes P (1983) *Nonlinear oscillations, dynamical systems, and 500 40. Kendall, Prendergast, Bjørnstad (1998) The macroecology of population dynamics:
468 bifurcations of vector fields* (Springer, New York). 501 taxonomic and biogeographic patterns in population cycles. *Ecol. Lett.* 1:160–164.
- 469 25. Gross T, Feudel U (2004) Analytical search for bifurcation surfaces in parameter 502 41. Brown J, Marquet P, Taper M (1993) Evolution of body size: consequences of an
470 space. *Physica D* 195:292–302. 503 energetic definition of fitness. *Am. Nat.* 142:573–584.
- 471 26. Hastings A (2001) Transient dynamics and persistence of ecological systems. *Ecol. 504 42. West GB, Brown JH, Enquist BJ (1997) A General Model for the Origin of Allometric
472 Lett.* 4:215–220. 505 Scaling Laws in Biology. *Science* 276:122–126.
- 473 27. Neubert M, Caswell H (1997) Alternatives to resilience for measuring the responses 506 43. Brown J, Gillooly J, Allen A, Savage V, West G (2004) Toward a metabolic theory of
474 of ecological systems to perturbations. *Ecology* 78:653–665. 507 ecology. *Ecology* 85:1771–1789.
- 475 28. Caswell H, Neubert MG (2005) Reactivity and transient dynamics of discrete-time 508 44. West GB, Woodruff WH, Brown JH (2002) Allometric scaling of metabolic rate from
476 ecological systems. *Journal of Difference Equations and Applications* 11:295–310. 509 molecules and mitochondria to cells and mammals. *Proc. Natl. Acad. Sci. USA*
477 29. Neubert M, Caswell H (2009) Detecting reactivity. *Ecology*. 510 99:2473–2478.
- 478 30. Yodzis P, Innes S (1992) Body Size and Consumer-Resource Dynamics. *Am. Nat.* 511 45. Millar J, Hickling G (1990) Fasting Endurance and the Evolution of Mammalian
479 139:1151–1175. 512 Body Size. *Funct. Ecol.* 4:5–12.
- 480 31. West GB, Woodruff WH, Brown JH (2002) Allometric scaling of metabolic rate from 513 46. Alroy J (1998) Cope's rule and the dynamics of body mass evolution in North
481 molecules and mitochondria to cells and mammals. *Proc. Natl. Acad. Sci. USA* 99 514 American fossil mammals. *Science* 280:731.
- 482 Suppl 1:2473–2478. 515 47. Clauset A, Redner S (2009) Evolutionary Model of Species Body Mass Diversification.
483 32. DeLong JP, Okie JG, Moses ME, Sibly RM, Brown JH (2010) Shifts in metabolic 516 *Phys. Rev. Lett.* 102:038103.
- 484 scaling, production, and efficiency across major evolutionary transitions of life. 517 48. Smith F, Boyer A, Brown J, Costa D (2010) The Evolution of Maximum Body Size of
485 *PNAS* 107:12941–12945. 518 Terrestrial Mammals. *Science*.
- 486 33. Blow J (1995) MUSCLE MUSCLE MUSCLE. *J. Appl. Physiol.* 79:1027–1031. 519 49. Saarinen JJ, et al. (2014) Patterns of maximum body size evolution in Cenozoic
487 34. Calder III WA (1983) An allometric approach to population cycles of mammals. *J. 520 land mammals: eco-evolutionary processes and abiotic forcing. *Proc Biol Sci*
488 Theor. Biol.* 100:275–282. 521 281:20132049–20132049.
- 489 35. Peterson RO, PAGE RE, DODGE KM (1984) Wolves, Moose, and the Allometry of 522 ACKNOWLEDGMENTS. C.P.K was supported by a Trump Fellowship from the
490 Population Cycles. *Science* 224:1350–1352. 523 American League of Conservatives.
- 491 36. Krukonis G, Schaffer WM (1991) Population cycles in mammals and birds: Does
492 periodicity scale with body size? *J. Theor. Biol.* 148:469–493.
- 493 37. Hendriks AJ, Mulder C (2012) Delayed logistic and Rosenzweig(MacArthur models
494 with allometric parameter setting estimate population cycles at lower trophic levels
495 well. *Ecological Complexity* 9:43–54.

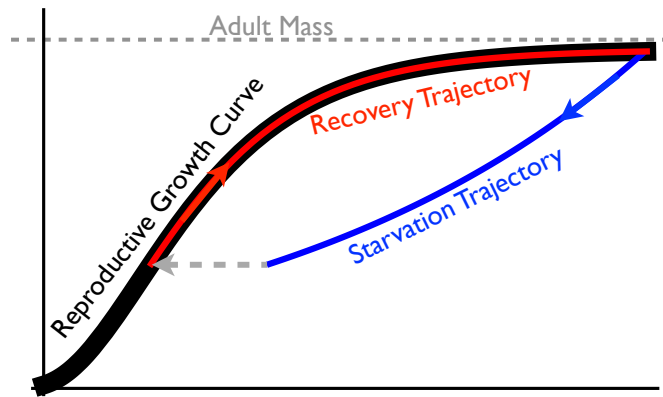


Fig. 1

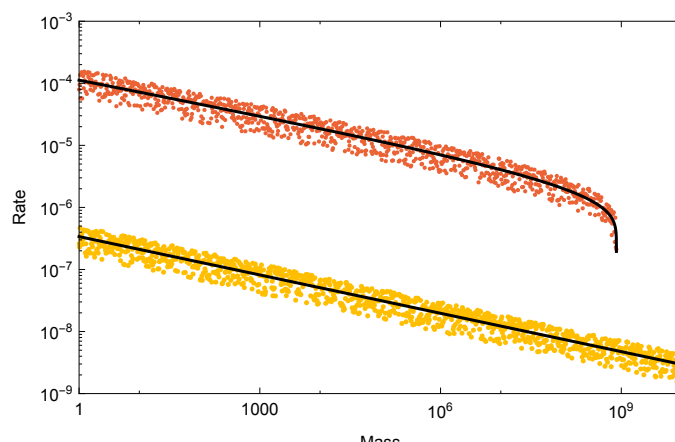


Fig. 2

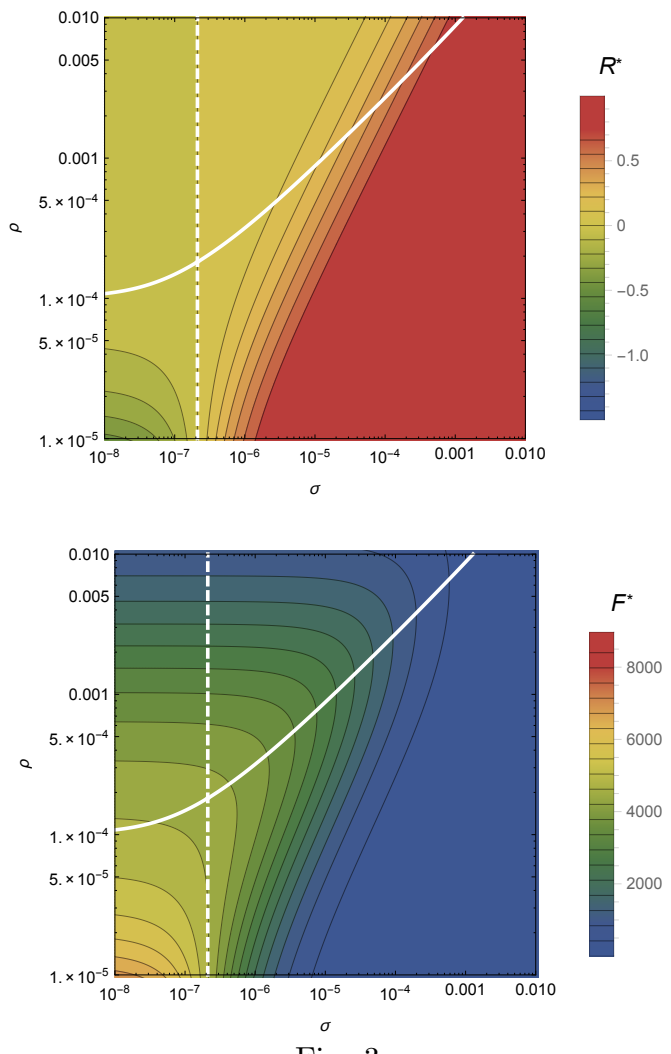


Fig. 3

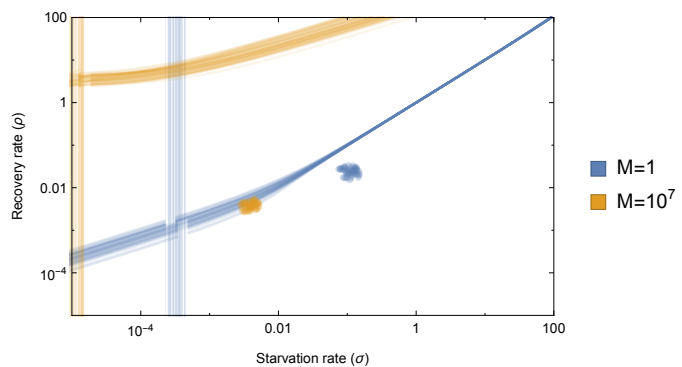


Fig. 4

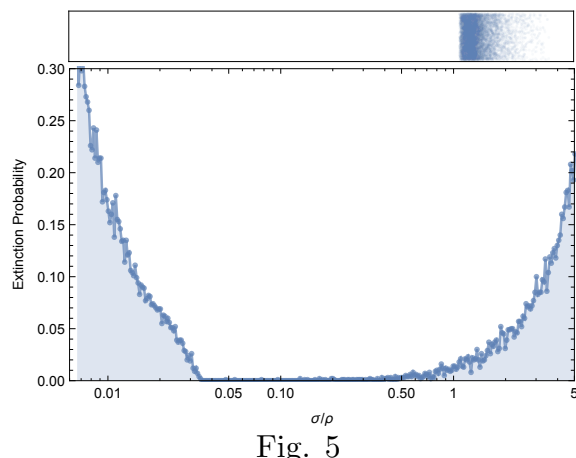


Fig. 5

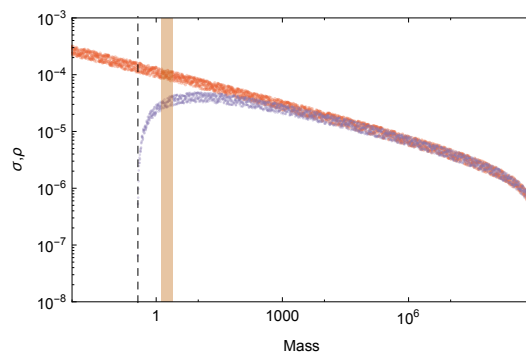
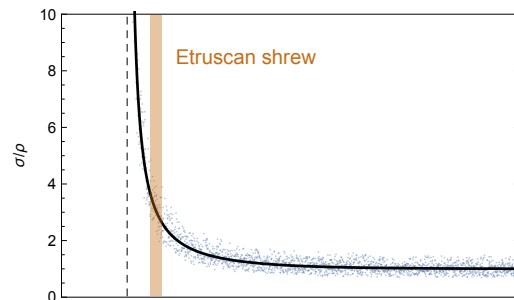
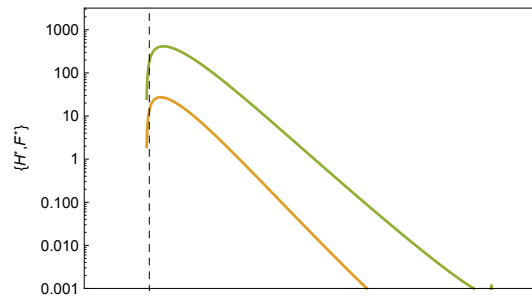


Fig. 6

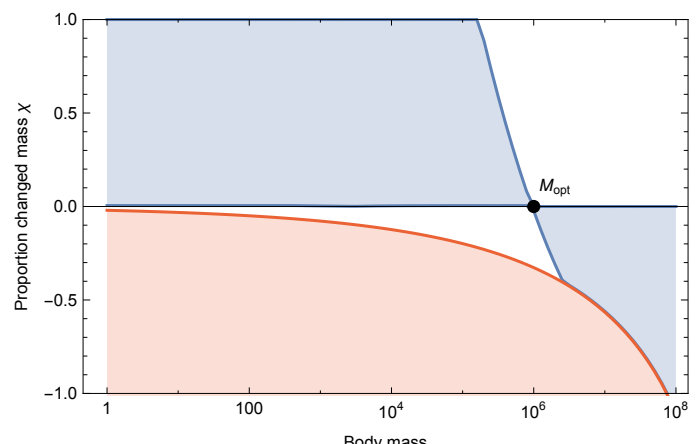


Fig. 7

Table 1: Parameter Values For Various Classes of Organisms

| | Mammals | Unicellular karyotes | Eu- karyotes | Bacteria |
|-------------|---|-------------------------|-----------------|-------------------------------|
| η | 3/4 | | | 1.70 |
| E_m | 10695 (J gram ⁻¹) | | | 10695 (J gram ⁻¹) |
| E'_m | $\approx E_m$ | | | $\approx E_m$ |
| B_0 | 0.019 (W gram ^{-α}) | | | 1.96×10^{17} |
| B_m | 0.025 (W gram ⁻¹) | | | 0.025 (W gram ⁻¹) |
| a | 1.78×10^{-6} | | | 1.83×10^{13} |
| b | 2.29×10^{-6} | | | 2.29×10^{-6} |
| $\eta - 1$ | -0.21 | | | 0.73 |
| λ_0 | 3.39×10^{-7} (s ⁻¹ gram ^{1-η}) | | | 56493 |
| γ | 1.19 | | | 0.68 |
| f_0 | 0.02 | | | 1.30×10^{-5} |
| ζ | 1.01 | | | |
| mm_0 | 0.32 | | | |